# MODELING BOREHOLE STONELEY WAVE PROPAGATION ACROSS PERMEABLE IN-SITU FRACTURES

by

X.M. Tang

New England Research, Inc.
76 Olcott Drive
White River Junction, VT 05001

C.H. Cheng

Earth Resources Laboratory
Department of Earth, Atmospheric, and Planetary Sciences
Massachusetts Institute of Technology
Cambridge, MA 02139

F.L. Paillet

U.S. Geological Survey
Box 25046 M.S. 403
Denver, CO 80225

## ABSTRACT

The characterization of hydraulic transmissivity of permeable fracture reservoirs is a very important task in the exploration of water resources and hydrocarbons. Previous studies that model the permeable structure as a single fluid-filled fracture failed to explain the observed significant Stoneley wave attenuation across the permeable structure. In this paper, the structure is modeled as a permeable fracture zone and synthetic Stoneley wave seismograms in the vicinity of the structure are calculated. The results show that Stoneley waves can be strongly attenuated or even eliminated without significant reflection, because of the dissipation of wave energy into the permeable zone. Several field cases are also modeled and the theoretical results are compared with the field data. It is shown that low- and medium-frequency Stoneley waves (1 kHz data from Moodus, Conneticut, and 5 kHz data from Monitoba, Canada) are very sensitive to the permeability of the fractures and can be used to assess permeability from in-situ logging data, if the fracture porosity and zone thickness can be measured. At high frequencies, however, Stoneley waves are not very sensitive to permeability but are mainly affected by the sum of the fracture openings expressed as the product of fracture zone thickness

and porosity in the fracture zone. This finding is demonstrated by a logging data set (Monitoba, Canada) obtained using high-frequency Stoneley waves at 34 kHz.

## INTRODUCTION

Permeable fractures in reservoirs are of major importance in assessing the fluid transport capacity of a well penetrating the reservoir. Full waveform acoustic logging has been used as an important means in the detection and characterization of borehole fractures. Through field observations, Paillet (1980) was able to recognize the effects of fractures intersecting the borehole on the logging waveforms. Since then, studies based on field data (Hsu et al., 1983; Arditty and Staron, 1987; Hardin et al., 1987; Brie et al., 1988), theoretical modeling (Bhashvanija, 1983; Stephen et al., 1985; Tang and Cheng, 1988; Hornby et al., 1989), and ultrasonic laboratory models (Güler and Toksöz 1987; Lakey, 1985; Poeter, 1987; Hornby et al., 1989) have been used to relate acoustic log characteristics to fracture properties. All studies show that full waveform acoustic logs are attenuated by fractures. The magnitudes of attenuation have been different. The field results show significant attenuation in some cases and little attenuation in others. Theoretical results, obtained using different techniques and different assumptions in formulating the problem, have yielded different results. Paillet et al. (1989) reviewed the existing theoretical models. Mathieu (1984) formulated the problem of Stoneley wave attenuation across a plane-parallel fracture by assuming that the fluid flow in the fracture is governed by viscous diffusion mechanism and that the conduction of fluid obeys the cubic law (Snow, 1965). However, Tang and Cheng (1988) studied the dynamic fluid flow in a fracture and show that the effect of viscosity is minimal at logging frequencies. Hornby et al. (1989) calculated the transmission and reflection of Stoneley waves at a plane fracture by omitting the viscous effects. Laboratory experiments with the plane fracture model (Tang and Cheng 1988; Hornby et al. 1989) have yielded results that agree with the theoretical results. Although both attenuation and reflection of Stoneley waves are predicted by the plane-fracture model, it takes a rather large fracture aperture (on the order of centimeters) to produce significant Stoneley wave attenuation. Fractures with such apertures are rarely found in the field (Hornby et al., 1989), but up to 50% or more Stoneley wave attenuation across *in situ* fractures is commonly observed (Paillet, 1980; Hardin et al., 1987). This discrepancy led Paillet (1989) to suggest that *in situ* fractures may consist of an array of flow passages and that fracture permeability is not directly related to the aperture of a plane-parallel fracture. In this study, we further substantiate this hypothesis by modeling fractures as a permeable zone in the formation. As will be shown, the permeable fracture zone model predicts that reflections are generated at the fracture zone and Stoneley wave attenuation across the fracture zone can be very significant, as observed field measurements.

## THEORY

Tang and Cheng (1991) recently developed a theory for calculating Stoneley wave propagation across heterogeneous and permeable borehole structures. The structure is modeled as a zone sandwiched between two formations of different properties. The theory is able to handle a variety of structures including a fluid-filled plane fracture (horizontal or inclined), an elastic layer, a permeable porous zone, and a permeable fracture zone. Detailed description of the theory is referred to the original article. In this study, we concentrate on the problem of a permeable fracture zone. We briefly outline the major steps concerning the calculation of a permeable fracture zone. This zone is modeled as thin layer of of porous materials which can have very high porosity and permeability. Figure 1 illustrates the configuration of the borehole, a logging (modeled as rigid), the permeable zone, and the surrounding formations. As the Stoneley wave encounters the permeable zone, interaction between borehole fluid and permeable fracture zone occurs because of dynamic fluid conduction into the permeable zone. This interaction is governed by the wave propagation characteristics in the zone as well as in the formation. Therefore, the interaction is characterized by two wavenumbers $k_1$ and $k_2$, where $k_1$ is the Stoneley wavenumber in the surrounding formation (i.e., the incident Stoneley wavenumber) that can be calculated using the borehole period equation (Tang and Cheng, 1991). The Stoneley wavenumber in the permeable zone $k_2$ can be calculated using Biot-Rosenbaum model (Rosenbaum, 1974; Cheng et al., 1987). However, this model is somewhat complicated. By applying the concept of dynamic permeability of Johnson et al. (1987) to acoustic logging in a porous formation, Tang et al. (1990) and Tang and Cheng (1991) showed that the the complicated Biot-Rosenbaum model can be much simplified to give an explicit expression for the Stoneley wavenumber.

$$k_2 = \sqrt{k_{etl}^2 + \frac{2Ri\rho_0\omega\kappa(\omega)}{(R^2-a^2)\mu}\sqrt{-\frac{i\omega}{D}+k_{etl}^2}\frac{K_1(R\sqrt{-i\omega/D+k_{etl}^2})}{K_0(R\sqrt{-i\omega/D+k_{etl}^2})}} \quad , \tag{1}$$

with

$$D = \frac{\kappa(\omega)K_f}{\phi\mu(1+\xi)} \quad ,$$

where $K_f$, $\rho_0$, and $\mu$ are pore fluid bulk modulus, density, and viscosity of the zone, $\phi$ is fracture porosity, $\xi$ is a correction for elasticity of the solid matrix (see Tang et al., 1990), $K_0$ and $K_1$ are the second kind modified Bessel functions of order zero and one, and $R$ and $a$ are the borehole and tool radii, respectively. The symbol $k_{etl}$ is an 'equivalent elastic' Stoneley wavenumber with a rigid tool in the borehole. It is calculated using the borehole period equation with the effective density and moduli (or velocities) of the fluid-saturated permeable zone. If the density and velocities are given for the dry rock, they can be converted to the fluid-saturated properties using Gasmann's equation (White, 1983). A critical parameter in Eq. (1) is the dynamic permeability given as

(Johnson et al., 1987)

$$\kappa(\omega) = \frac{\kappa_0}{\left(1 - \frac{i\alpha\kappa_0\rho_0\omega}{3\mu\phi}\right)^{1/2} - \frac{i\alpha\kappa_0\rho_0\omega}{\mu\phi}} \quad , \tag{2}$$

where $\kappa_0$ is the static Darcy permeability, $\alpha$ is the high-frequency limit of the dynamic tortuosity, which is a parameter describing the tortuous, winding pore space. If the flow channels are straight (fractures), $\alpha$ is taken to be 1. The dynamic permeability captures the frequency-dependence of fluid flow in porous media and makes the simplified theory (Eq. 1) consistent with the exact theory of Biot-Rosenbaum model (Rosenbaum, 1974, Cheng et al., 1987) even at high frequencies (Tang et al., 1990). The transmission and reflection coefficients at the permeable zone are given by (Tang and Cheng, 1991)

$$TC = \frac{4k_1k_2e^{-ik_2L}}{(k_1+k_2)^2e^{-ik_2L} - (k_1-k_2)^2e^{ik_2L}} \quad , \tag{3}$$

$$RC = \frac{2i(k_2^2-k_1^2)\sin(k_2L)}{(k_1+k_2)^2e^{-ik_2L} - (k_1-k_2)^2e^{ik_2L}} \quad , \tag{4}$$

where $L$ is the thickness of the permeable zone. In addition to the transmission and reflection coefficients, Tang and Cheng (1991) have also obtained solutions for Stoneley wave motion in the permeable zone. As a result, synthetic seismograms can be computed for any source-receiver locations, which can be used to simulate the Stoneley wave log across the permeable zone.

## APPLICATION TO FIELD DATA

We have presented a theory for calculating Stoneley wave propagation across borehole fractures. We now apply the theory to study the Stoneley wave log data across in-situ fractures. In practice, acoustic logging is performed in a very broad frequency range, from 200 Hz up to 35 kHz (Hornby et al., 1989; Paillet, 1980). Because the fracture fluid motion excited by logging acoustic waves is dynamic in nature (Johnson et al., 1987; Tang and Cheng, 1988), it is expected that the model that accounts for the dynamic effects will have different responses in the different frequency ranges. In the following, three different data sets will be employed. They span the low, medium, and high frequency ranges of the theory. This allows us to explore the theory in the full frequency range and to see how the flow properties of fractures affect the measured wave characteristics in the different frequency ranges.

## Data From Moodus #1 Well (Low Frequency Range)

We apply the permeable zone theory to the modeling of the Stoneley (tube) wave log across a fracture zone in the Moodus #1 well drilled in east-central Connecticut. The well was drilled into crystalline rocks. A major water-producing zone at a depth of about 610 ft was identified. The various log data in the vicinity of the zone have been published in the 1989 SPWLA symposium (Hornby et al., 1990) and are re-presented in Figure 2. Of special interest is the Stoneley wave log in Figure 2a. This log was recorded using a research prototype sonic tool which excites a Stoneley wave with centerband energy around 1 kHz (Hornby et al., 1990). As seen from Figure 2a, Stoneley wave reflections are clearly generated at the fracture zone. The reflection coefficient of about 0.1 was estimated (Figure 2a). In the section across the zone (at the origins of the up- and down-going reflected waves) the transmitted waves show weaker amplitudes compared with the waves outside the section. In other words, Stoneley waves are attenuated across the zone. The borehole televiewer in Figure 2b shows that the thickness of the zone is about 5 ft. The fracture image obtained using the Formation Microscanner indicates that the zone consists a large number of micro-fractures and the average fracture porosity is on the order of 10%. Although fracture porosity determined by an electrical tool is usually very variable, this porosity value can still be used as an order-of-magnitude estimate for the fracture zone. This data set presents a very good example for our theoretical modeling. It also provides most of the parameters needed for the modeling. The borehole radius is given in Figure 2a as $R$ =8.5 cm. We assume that the tool radius is $a$ =0.4 cm. Since the well is in crystalline rocks, we assume that the density, compressional and shear velocities are $\rho$=2.7 kg/m$^3$, $V_p$=6 km/s, and $V_s$=3 km/s. The same parameters are also used for the rock matrix of the fracture zone. For the fracture zone, we use a porosity of $\phi$=10% (Figure 2b) and the tortuosity $\alpha$ in Eq. (2) is assumed to be 1. The zone and the borehole are filled with water whose density, acoustic velocity, and viscosity are $\rho_0$=1 kg/m$^3$, $V_f$=1.5 km/s, $\mu$=1 cp. The zone thickness $L$ in Eq. (2) is 1.52 m ($\approx$ 5 ft). The only uncertain parameter in the modeling is the permeability $\kappa_0$ in Eq. (3). Fortunately, we have the measured Stoneley wave reflectivity (Figure 2a). The permeability can then be estimated by matching the theoretical reflection coefficient with the measured value.

Using Eq. (4) and the given parameters, we have calculated the reflection coefficient for a number of permeability values. The results are shown in Figure 3. As pointed out by Tang and Cheng (1991), the reflection calculated using Eq. (4) represents the superposition of the reflections from the top and bottom interfaces of the zone. Because of the low-frequency signal used in the present case, the two reflections are indistinguishable in the time domain and we have to consider their total effects. However, for the permeable zone the contribution from the bottom reflection will be reduced because of the attenuation of the reflection during its propagation through the zone. For the $\kappa_0$=1 Darcy curve of Figure 3, the attenuation is not very strong, so that the superposition

of the two reflections results in the undulation of the reflection curve. For the $\kappa_0$=10 Darcy curve, the bottom reflection is almost completely attenuated and the curve represents primarily the top reflection which has no undulation. Thus the reflection curve is quite sensitive to the permeability of the zone. Around 1 kHz which is the measurement frequency, the 1 Darcy curve gives a too low reflectivity while the 10 Darcy curve gives a too high value. The $\kappa_0$=4 Darcy curve gives an average reflectivity of 0.1 between 0.5 and 1.5 kHz. This $\kappa_0$ value is thus chosen as the representative permeability of the fracture zone.

Hornby et al. (1990) interpreted the data in Figure 2 in terms of the plane fracture theory (Hornby et al., 1989). They attributed the observed Stoneley reflection to an equivalent parallel plate fracture with an aperture of 5.6 mm, which gives a reflectivity of 0.1 around 1 kHz. This aperture was obtained with a fluid-filled borehole. If a rigid tool of 4 cm radius in the borehole is accounted for, the aperture value reduces slightly to 4.5 mm, which gives the same reflectivity of 0.1 around 1 kHz. It is convenient here to compare the full results from the present theory and the plane fracture theory. To do this, we have computed synthetic Stoneley wave logs across the fracture zone using the two theories. The seismograms are calculated using a Kelly source (Kelly et al., 1976) with a center frequency of 1 kHz. The source-receiver spacing is 3.06 m (Hornby et al., 1990). Figures 4 and 5 show the results. The seismograms in Figure 4 are computed using the permeable zone theory, while those in Figure 5 are using the plane fracture of 4.5 mm. The two separate figures show the same features for the up- and down-going reflected waves, the amplitudes of these waves being almost equal. However, the waves transmitted across the fracture zone, as indicated by arrow(s) in the figures, are quite different. The permeable zone theory predicts significant attenuation for the transmitted waves, whereas the plane fracture theory shows very slight attenuation.

The Stoneley log data (Figure 2a) exhibit significant attenuation, as can be seen from the distortion and thinning of the direct waves in the vicinity of the fracture zone. For a further comparison, Figure 6 plots the transmission and reflection coefficients for the permeable zone theory (solid curves) and the plane fracture theory (dashed curves) in the frequency range of 0–2 kHz. The reflection curves from the two theories match quite well and predict a reflectivity of about 0.1 around 1 kHz. However, the transmission curves from the two theories differ greatly. Around 1 kHz, the permeable zone theory predicts a transmission coefficient of 0.28, while the plane fracture theory gives a value of 0.9. This latter value cannot explain the significant attenuation on the Stoneley wave log of Figure 2a. This comparison shows that in the presence of a fracture zone, permeability or fluid transmissivity, rather than the equivalent fracture aperture, is the appropriate parameter to characterize the fractures. The modeling example presented here also indicates that the permeable zone theory can be used in conjunction with borehole images, lithology indicators, and other log data to characterize the overall fluid transport properties of a fracture zone. Unfortunately, Stoneley wave transmission is not available from this data set, although it could have been measured. The transmitted

waves provide a constraint on the parameter estimation and a robust estimate of the fracture flow properties.

## Data From URL-M11 Well (Medium Frequency Range)

We now study the data set obtained in a borehole (M11 well) at the Underground Research Laboratory (URL) located on the southern edge of the Canadian shield in southeastern Manitoba, Canada. A major isolated fracture was detected at a depth of 187 m in this borehole. Figure 7 shows the televiewer log, the Stoneley waveform data, and the Stoneley amplitude log data in the vicinity of the fracture. This isolated fracture appeared as a single subhorizontal band on the televiewer log, but additional high-resolution televiewer logs indicated that this one feature was actually composed of several subparallel fractures. The waveforms were obtained using a sparker source at 5 kHz, a much higher frequency than the frequency (1 kHz) of the previous Moodus #1 well case. This frequency lies in the medium frequency range of acoustic logging using Stoneley waves, although still somewhat lower than the frequencies used in conventional sonic logging. The borehole and the tool diameters were 15.2 and 5.1 cm, respectively. The source-receiver spacing was 2.14 m. The Stoneley waves are significantly attenuated across the fractures. A Stoneley wave reflection at the top can also be observed, as indicated by the line in Figure 7, which marks the moveout of the reflected waves. The Stoneley attenuation is measured as the amplitude deficit or transmission loss across the fractures. This measurement has long been used in fracture detection and characterization (Paillet, 1980). To compute the attenuation, one first applies a window that contains Stoneley arrivals. Then the mean square wave energy (sum of the square of each sampled wave amplitude within the window) is computed and is multiplied by a Half cosine filter. The attenuation or transmission loss is measured from the amplitude deficit – the "representative" percentage decrease of average wave energy in the time window over the vertical distance of one source-receiver separation. The transmission loss obtained in this way gives a measure for the square of transmission coefficient around the measurement frequency, which will be demonstrated with a synthetic example.

The characteristics of the Stoneley waves in the vicinity of the fractures can now be modeled. The tool and bore radii as well as source-receiver spacing have already been given as above. According to Paillet (1984), the formation parameters are $V_p$=5.8 km/s, $V_s$=3.3 km/s, and $\rho$ = 2.65 kg/m$^3$. The borehole and fracture saturant fluid is water with $V_f$=1.5 km/s, $\rho_0$=1 kg/m$^3$, and $\mu$=1 cp. The thickness of the zone is taken to be the width of the blackened band on the televiewer log. It is about 0.4 m. The width of the anomaly on the amplitude log (Figure 7) also gives a measure of the zone thickness. The opening of the anomaly is about 2.6 m. Subtracting the source-receiver spacing (2.14 m) from it gives a thickness of 0.46 m, not far from that measured from the televiewer image. We assume that the fluid-saturated zone is filled with some softer materials with $V_p$=3 km/s, $V_s$=2 km/s, and $\rho$= 2.1 kg/m$^3$. By assuming that flow

takes place along fractures, we can set $\alpha$ to 1. Unlike the previous Moodus #1 well case where the fracture porosity $\phi$ was supplied, we have two uncertain parameters, $\kappa_0$ and $\phi$ in the present case. The values of $\kappa_0$ and $\phi$ are tentatively estimated by fitting the amplitude log data on Figure 7. From this fit, we obtain a pair of the parameters as $\kappa_0$=2.5 Darcies and $\phi$=35%. With these parameters, synthetic iso-offset seismograms are calculated and the results are shown in Figure 8. The source centerband frequency is 5 kHz. The calculated Stoneley wave attenuation and reflection are very similar to those observed in Figure 7. The calculated amplitude deficit log (solid line) on the left matches the measurement (open circles) quite well. Both logs show an average deficit of about 82% across the zone. It is also interesting to note that both the synthetic and measured logs show a slight amplitude increase at the top fracture zone surface, as indicated on the logs of Figure 8. This effect is due to the constructive interference of the (small) reflected wave with the incident wave at the top interface.

To better illustrate the Stoneley transmission and reflection, Figure 9 plots the calculated transmission and reflection coefficients in the frequency range of 0-10 kHz. Around 5 kHz, the transmission coefficient is about 0.43, which gives an amplitude deficit value of about $[1-(0.43)^2]\times 100\% \approx 82\%$, in agreement with the value given in Figure 8. The average reflection coefficient from 4 to 6 kHz is about 0.12. A rough estimate from the waveform data in Figure 7 gives a value of about 0.15. The two values are of the same order. However, the theoretical reflection value contains contributions from both the permeability effect and the lithology effect due to the assumed 'softer' fracture zone material properties. This value could still be increased if we use even lower velocities and density for the zone. On the other hand, if the elastic parameters of the fracture zone are close to those of the formation, the reflection coefficient would reduce to only about 0.06, which is primarily due to the fracture permeability effect. This supports the suggestion by Paillet (1984) that the significant reflection in Figure 7 could be due to both the effect of fracture permeability and the effect of lithology changes associated with altered rock in the fracture zone. One can also notice that the field data shown in Figure 7 do not have a clearly traceable down-going reflection. This could probably be due to the fact that the bottom part of the zone may be less permeable and altered than the top part. It can be seen from the amplitude data (Figure 8) that the top of the fracture zone is very sharp, while the amplitude decrease at the bottom is more gradual. This helps explain why the reflection is seen clearly at the top but not the bottom. The synthetic log shows that the amplitude change at the bottom is also sharp, because this gradual change is not modeled in the theory. Although in general the theory models the field data fairly well, we caution the reader that the estimated $\kappa_0$ and $\phi$ may not be unique, because the transmission datum at one single frequency is not sufficient to constrain the two model parameters. Other choices of $\kappa_0$ and $\phi$ (say, decrease $\phi$ and increase $\kappa_0$) may also fit the data. The purpose of this modeling was not to estimate the flow properties of the fracture zone, but rather to demonstrate that with reasonable model parameters, the permeable zone theory can correctly model the Stoneley wave characteristics in the vicinity of a fracture zone.

## Data From Manitoba Fracture Data Set (High Frequency Range)

As a final example of this study, we apply our permeable zone theory to study the fracture log data obtained from an experimental well drilled on the grounds of the Whiteshell Nuclear Research Establishment located near Pinawa, Manitoba, Canada. The well was surveyed using a borehole televiewer and an acoustic sonde. A series of fractures were detected at depths from 395 to 460 m. Packer isolation and injection tests were also carried out to measure the fracture permeability. Figure 10 shows the Stoneley wave amplitude log and televiewer log for the depths (original results were given in Paillet, 1980). The Stoneley amplitude deflections correspond to the televiewer fracture images very well. On the same figure, results from the three measurements are also compared. They are:

1. Maximum Stoneley wave amplitude reduction opposite the fracture.
2. Fracture width visually measured from the televiewer.
3. Effective fracture permeability determined by packer isolation and injection tests.

All three traces are described in terms of the percentage of maximum value measured in this interval. We can now use our theory to model the measured Stoneley amplitude reduction on the measured amplitude log. The formation and borehole fluid properties are assumed to be the same as those used for the URL-M11 well. The elastic parameters of the zone are taken as the same as those of the formation. The source-receiver spacing is 0.6 m and the borehole and tool (steel body) radii are 3.5 and 2.5 cm, respectively (Paillet, 1980). Because the waveguide now is a thin cylindrical shell of 1 cm thick, the Stoneley can be excited at a fairly high frequency (34 kHz). This happens because the source frequency is below the cut-off frequency of the lowest borehole pseudo-Rayleigh mode, so that Stoneley wave are the only waveguide mode excited in the borehole. Of most importance are the parameters of the permeable zones. As before, the tortuosity $\alpha$ can be set to 1. As demonstrated in the URL-M11 well example, the thickness of the zone $L$ can be estimated from the width of the anomalies on the Stoneley amplitude log. The width is measured as the opening of the anomalies on the base line of the amplitude log. The thickness $L$ is obtained by subtracting the source-receiver spacing (0.6 m) from the measured width. The estimated $L$ values for the fracture zones are given on the synthetic log in Figure 10. The permeability values can be assessed from the packer test results. In fact, the absolute permeability values are not important for this high-frequency logging data at 34 kHz, as can be seen from the dynamic permeability given in Eq. (2), when $\omega \to \infty$, $\kappa(\omega) \to i\mu\phi/(\alpha\rho_0\omega)$, independent of $\kappa_0$. Therefore, according to the permeable zone theory, the attenuation seen in Figure 10 is not sensitive to the $\kappa_0$ values. Rather, it is sensitive to the fracture porosity $\phi$. We therefore determine the $\kappa_0$ values by assigning a $\kappa_0$ value at one particular fracture zone, say $\kappa_0$=0.46 Darcy at the zone occurring at 395 m, and then computing other $\kappa_0$ values according to the relative

values from the packer test results given on Figure 10. The only parameter which needs to be known is fracture porosity $\phi$. It is determined by fitting the theoretical Stoneley amplitude deficit with the measured value given in Figure 10. Note that in the calculation for the very thick zone at 395 m, the parameter $L$ in Eq. (3) is not the zone thickness of 3.6 m, but the source-receiver spacing of 0.6 m, this spacing being the maximum travel distance of a Stoneley wave when the source and receiver are both in the thick zone.

After estimating the parameters needed to define the fracture zone model, synthetic iso-offset Stoneley seismograms across each zone were calculated and the synthetic amplitude log computed in the same way as for the field data. The synthetic log compares well with the measured Stoneley wave amplitude log. The calculated $\phi$ value for each fracture zone is given on the synthetic log. Since the formation is a non-porous crystalline rock (granite), the estimated porosities of a few percent are significant enough to indicate the existence of the fractures. For the very thick fracture zone ($L$=3.6 m) at 395 m, the calculated $\phi$ value is 3%. This value is small compared with the value of $\phi$=12% for the thin zone ($L$=0.07 m) at about 430 m. However, since the multiple interconnected fracture zone at 395 m is so thick that the source and receiver are both submerged in the zone, the integrated effect attenuates the Stoneley waves almost completely. Again, this modeling shows that with reasonable model parameters, the permeable zone model accounts for the observed Stoneley wave attenuation across fractures.

The reliability and significance of the estimated parameters $\kappa_0$, $L$, and $\phi$ are now analyzed. Because of the very high frequency of this data set, the model has very little sensitivity to permeability, as discussed before. In fact, we have computed the synthetic amplitude log of Figure 10 by increasing the permeability numbers on this figure by a factor of 10. The calculated log stays almost the same. Thus the permeability numbers in Figure 10 are not very meaningful. They are used only for model initiation. However, an important finding here is that the product $L\phi$ is a fairly robust and reliable quantity to estimate. It has an almost one-to-one correspondence to the measured amplitude deficit in Figure 10. In terms of the permeable zone theory, the deficit around a frequency (34 kHz) can be expressed as one minus the square of the transmission coefficient (Eq. 3) evaluated at the frequency (i.e., $1-|TC|^2$). Although Eq. (3) relates the model parameters in a complicated way, the dominate contribution comes from the controlling factor $\exp(-ik_2L)$, whose high frequency behavior can be readily analyzed. Taking the high frequency expression of the dynamic permeability (Eq. 2), it can be shown that $D$ in Eq. (1) is independent of both $\kappa_0$ and $\phi$, and $k_2$ given in Eq. (1) becomes

$$k_2 = \sqrt{k_{etl}^2 - \frac{2\phi R}{\alpha(R^2-a^2)}F(\omega)} \quad , \tag{5}$$

where $F(\omega)$ is an expression that is independent of $\kappa_0$, $\phi$, as well as the fluid viscosity $\mu$. Physically, this means that at high frequencies, the viscous skin depth $\delta = (2\mu/\rho_0\omega)^{1/2}$

becomes much smaller than the aperture of the flow channels, and the flow resembles the potential flow of an electrical current that is sensitive only to the geometry (controlled by $\alpha$) and volume (given by $\phi$) of the flow channels (for water, $\delta$ is only about 3 $\mu$m at 34 kHz). In terms of the logging measurement, this suggests that *the high frequency Stoneley waves probe primarily the fluid-saturated volume (given by $\phi$) of the fracture zone.* The transmission loss or attenuation due to the permeable zone is mainly controlled by the imaginary part of $k_2$, this part being given by the second term under the square root sign in Eq. (5). Taking the first order expansion of Eq. (5) and noting that the attenuation is givne by $1 - |C\exp(-ik_2L)|^2$ (where $C$ is the square of the remaining part of Eq. 3),we obtain

$$\begin{aligned} \text{ATTENUATION} &= 1 - |C^2|\exp(-2L\text{Im}\{k_2\}) \\ &\approx 1 - |C^2|\exp\left[-(L\phi)\frac{2R}{\alpha k_{etl}(R^2-a^2)}\text{Im}\{F(\omega)\}\right] \quad , \end{aligned} \tag{6}$$

where $Im\{--\}$ denotes taking the imaginary part. This expression shows that the Stoneley transmission loss at high frequencies is an increasing function of the product of the zone thickness $L$ with the fracture porosity $\phi$.

The results given by Eq. (6) can be readily tested. Figure 11a plots the measured amplitude deficit (open squares) and the product $L\phi$ (solid squares) obtained from the modeling. The results of different units are scaled by their respective values at 413 m, so that the correspondence between attenuation and $L\phi$ can be examined. Again, for the very thick zone at 395 m, the parameter $L$ is the source-receiver spacing (0.6 m), instead of the zone thickness (3.6 m). As predicted, the measured attenuation corresponds to the estimated $L\phi$ value of each zone very well. This confirms our theoretical analysis. This result also has an important implication to acoustic logging measurements. In the case of very thin fracture zones (such as the ones between 420 and 440 m in Figure 10), the thickness $L$ may not be measured accurately and this results in the inaccuracy of the estimated fracture porosity $\phi$. However, the product $L\phi$ is constrained by the requirement to match the measured amplitude deficit. This means that the quantity $L\phi$ is a reliable parameter. Since $L\phi$ times $2\pi R$ is the total fluid area exposed to the borehole, this indicates that *the high frequency Stoneley wave transmission across a fracture zone measures the integrated effects of the fracture fluid layers, regardless of how these fractures are distributed across the zone.*

This result can also be derived from the study of dynamic fluid flow of a single fracture (Tang and Cheng, 1988). At very low frequencies, the fracture fluid conductivity $\bar{C}$ obeys the cubic law (Snow, 1965), i.e., $\bar{C} \propto L^3$. At high frequencies, the conductivity is linearly proportional to $L$ (Tang and Cheng, 1988), so that the transmission loss (which is nearly proportional to $\bar{C}$) due to different fractures are linearly summable. This also means that the effect of a stack of fracture fluid layers is comparable to the effect of a single fluid-filled fracture whose thickness is the sum of the thicknesses of the smaller fractures. This hypothesis can be tested numerically. For the fracture zones, the

thickness of the 'equivalent' single fracture is simply the $L\phi$ values given in Figure 11a, which are on the order of one centimeter. Using the plane-fracture theory of Hornby et al. (1989), the transmission loss can be calculated. In the calculation, however, the effects of the logging tool must be considered. This is done by replacing the borehole area with the area of the fluid annulus between the tool and the borehole wall. The calculated transmission loss is plotted in Figure 11b, against the measured values of each fracture zone. The predicted values match the measured values fairly well. Since the $L\phi$ values are derived from the measured attenuation using the permeable zone theory, we obtained a fair reconciliation between the permeable zone theory and the plane-fracture theory at high frequencies. However, for the explanation of the significant attenuation, the analogy of a single fracture is not appropriate since a fracture opening at centimeters is rarely found, whereas this value is quite reasonable for the sum of fracture apertures across a fracture zone. In addition, in calculating the synthetic seismograms (not shown) using the two theories, the plane-fracture theory shows a very significant reflection while the permeable zone theory shows no measurable reflections, simply because the acoustic impedance contrast between the solid formation and the thick fluid layer (single fracture) is much bigger than that between the formation and the saturated materials in the fracture zone.

## CONCLUSIONS

In this study, we have tested the new theoretical model for Stoneley wave propagation across permeable fractures by comparing it with field data. We have explored the theory in the full frequency range in which the fluid flow in fractures varies from viscous diffusion to dynamic wave motion. In all cases, the theoretical results are in good agreement with the field data. Application to the low-frequency data from the Moodus #1 well shows that the theory is very sensitive to permeability at low frequencies and can be used to assess fracture permeability from the measurement data. The medium-frequency data from the URL-M11 well showed that with reasonable choice of fracture permeability and porosity, the Stoneley wave characteristics in the vicinity of a fracture zone can be satisfactorily modeled. The case of high-frequency data from the Manitoba data set indicates that at very high frequencies, the model is controlled by the parameter $L\phi$, or the total fluid volume across the fracture zone. These examples demonstrate that the permeable zone model can be used as an effective method for fracture detection and characterization.

## ACKNOWLEDGEMENTS

We thank Brian Hornby for premitting us to use a figure from his original paper. This research was supported by New England Research, Inc., by the Full Waveform Acous-

tic Logging Consortium at M.I.T. and by the Dept. of Energy Grant No. DE-FG02-86ER13636.

## REFERENCES

Arditty, P.C. and P. Staron, 1987, Lithologic analysis and fracture detection in open and cased holes, Sonic Full Wave Research Workshop, *Soc. Expl. Geophys. 57th Ann. Mtg. and Exposition*, New Orleans, LA.

Bhashvanija, K., 1983, *A finite difference model of an acoustic logging tool: The borehole in a horizontal layered geologic medium*, Ph.D. Thesis, Colorado School of Mines, Golden, CO.

Brie, A., K., Hsu, and C. Eckersley, 1988, Using the Stoneley normalized differential energies for fractured reservoir evaluation; *Trans., Soc. Prof. Well Log Analysts, 29th Ann. Log. Symp.*, San Antonio, TX, XX1-XX25.

Cheng, C.H., J.Z. Zhang, and D.R. Burns, 1987, Effects of in-situ permeability on the propagation of Stoneley (tube) waves in a borehole, *Geophysics, 52*, 1297-1289.

Güler, F., and M.N. Toköz, 1987, Ultrasonic laboratory study of full waveform acoustic logs in boreholes with fractures, *M.I.T. Full Waveform Acoustic Logging Consortium Annual Report.*

Hardin, E.L., C.H. Cheng, F.L. Paillet, and J.D. Mendelson, 1987, Fracture characterization by means of attenuation and generation of tube waves in fractured crystalline rock at Mirror Lake, New Hampshire, *J. Geophys. Res., 92*, 7989–8006.

Hornby, B.E., D.L. Johnson, K.H. Winkler, and R.A. Plumb, 1989, Fracture evaluation using reflected Stoneley-wave arrivals, *Geophysics, 54*, 1274–1288.

Hornby, B.E., S.M. Luthi, and R.A. Plumb, 1990, Comparison of fracture apertures computed from electrical borehole scans and reflected Stoneley waves: an integrated interpretation, *Trans., Soc. Prof. Well Log Analysts, 31st Ann. Symp.*, Paper L.

Hsu, K., A. Brie, and R.A. Plumb, 1985, A new method for fracture identification using array sonic tools, *Rep. 14397*, Soc. of Petrol. Engineer.

Johnson, D.L., J. Koplik, and R. Dashen, 1987, Theory of dynamic permeability and tortuosity in fluid-saturated porous media, *J. Fluid Mech., 176*, 379-400.

Kelly, K.R., R.W. Ward, S. Treitel, and R.M. Alford, 1976, Synthetic microseismograms: A finite-difference approach, *Geophysics, 41*, 2–27.

Lakey, K.G., 1985, *Physical Modeling of the Full Acoustic Wave Train in a Borehole with a Perpendicular Fracture*, Master's Thesis, Washington State University, Pullman, Washington.

Paillet, F.L., 1980, Acoustic propagation in the vicinity of fractures which intersect a fluid-filled borehole, *Trans., Soc. Prof. Well Log Analysts, 21st Ann. Symp.*, Paper DD.

Paillet, F.L., and J.E. White, 1982, Acoustic modes of propagation in the borehole and their relationship to rock properties, *Geophysics, 47*, 1215–1228.

Paillet, F.L., 1984, Field test of a low-frequency sparker source for acoustic waveform logging, *M.I.T. Full Waveform Acoustic Logging Consortium Annual Report*, 207–228.

Paillet, F.L., C.H. Cheng, and X.M. Tang, 1989, Theoretical models relating acoustic tube-wave attenuation to fracture permeability – reconciling model results with field data, *Trans., Soc. Prof. Well Log Analysts, 30th Ann. Symp.*

Poeter, E.P., 1987, Characterizing fractures at potential nuclear waste repository sites with acoustic waveform logs, *Log Analyst, 28*, 453–461.

Rosenbaum, J.H., 1974, Synthetic microseismograms: logging in porous formations, *Geophysics, 39*, 14-32.

Snow, D.T., 1965, A parallel plate model of fractured permeability media, Ph.D. Thesis, Univ. of Calif., Berkeley, 1965.

Steven, R.A., F. Pardo-Casas, and C.H. Cheng, 1985, Finite difference synthetic acoustic logs, *Geophysics, 50*, 1588–1609.

Tang, X.M., and C.H. Cheng, 1988, A dynamic model for fluid flow in open borehole fractures, *J. Geophys., Res., 94*, 7567–7576.

Tang, X.M., C.H. Cheng, and M.N. Toksöz, 1990, Dynamic permeability and borehole Stoneley waves: A simplified Biot-Rosenbaum model, submitted to *J. Acoust. Soc. Am.*

Tang, X.M., and C.H. Cheng, 1991, Borehole Stoneley wave propagation across heterogeneous and permeable structures, M.I.T. Full Waveform Acoustic Logging Consortium Annual Report, this issue, 1991.

White, J.E., *Underground Sound*, Elsevier Science Publ. Co., Inc., 1983.

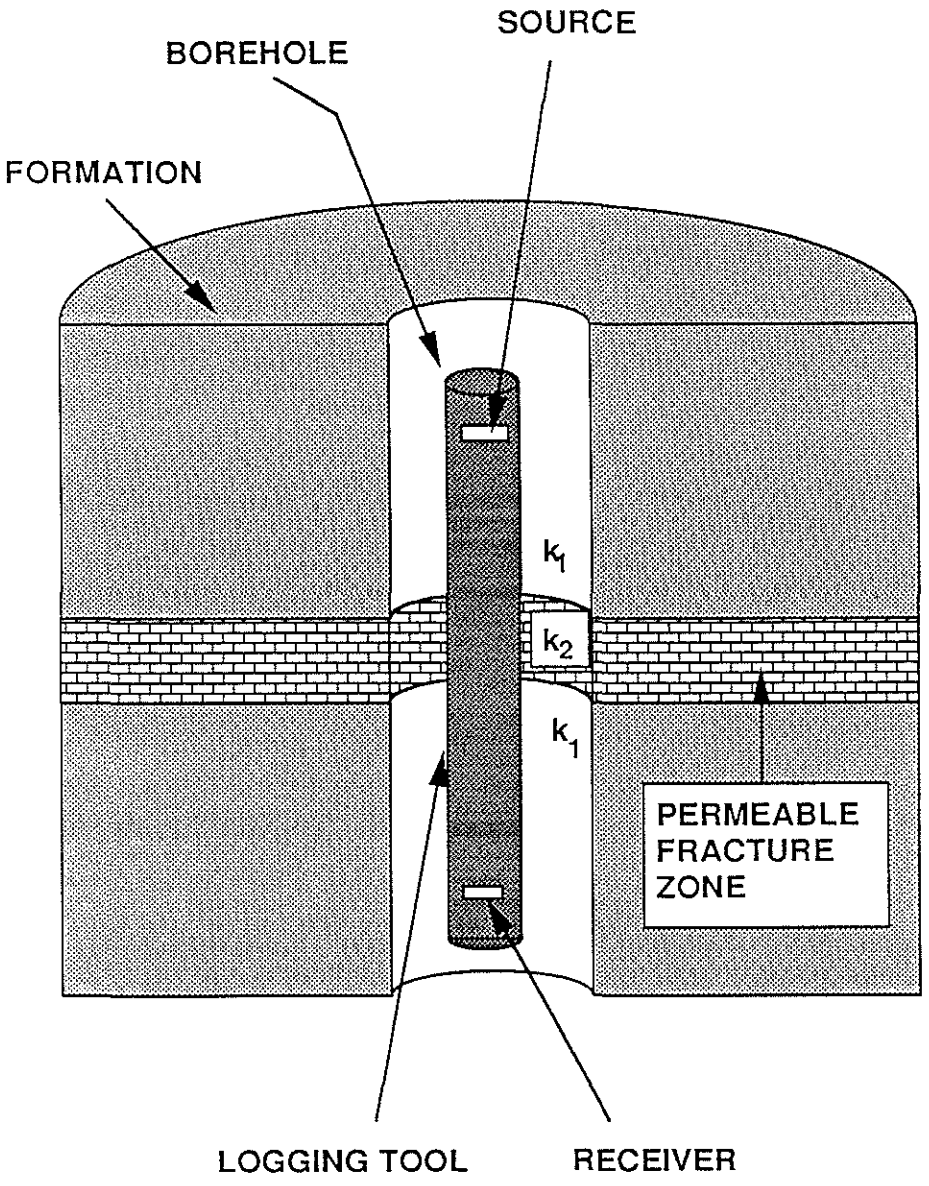


Figure 1: Diagram showing acoustic logging across a permeable borehole fracture zone. The interaction of the Stoneley wave and the zone is modeled as due to the different wavenumbers $k_1$ and $k_2$of the zone and formation.

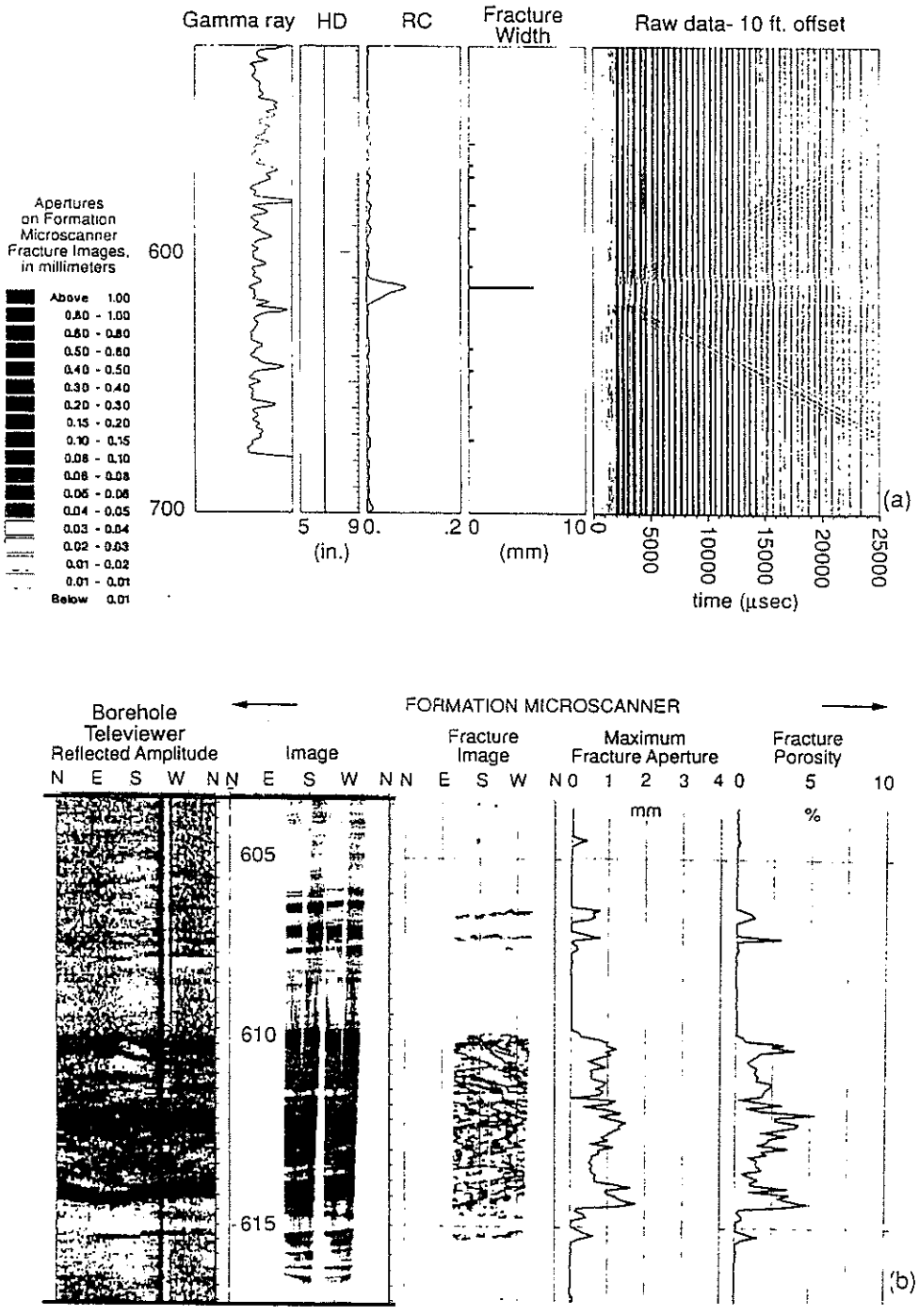


Figure 2: Various borehole logs for the Moodus #1 well (After Hornby et al., 1990).

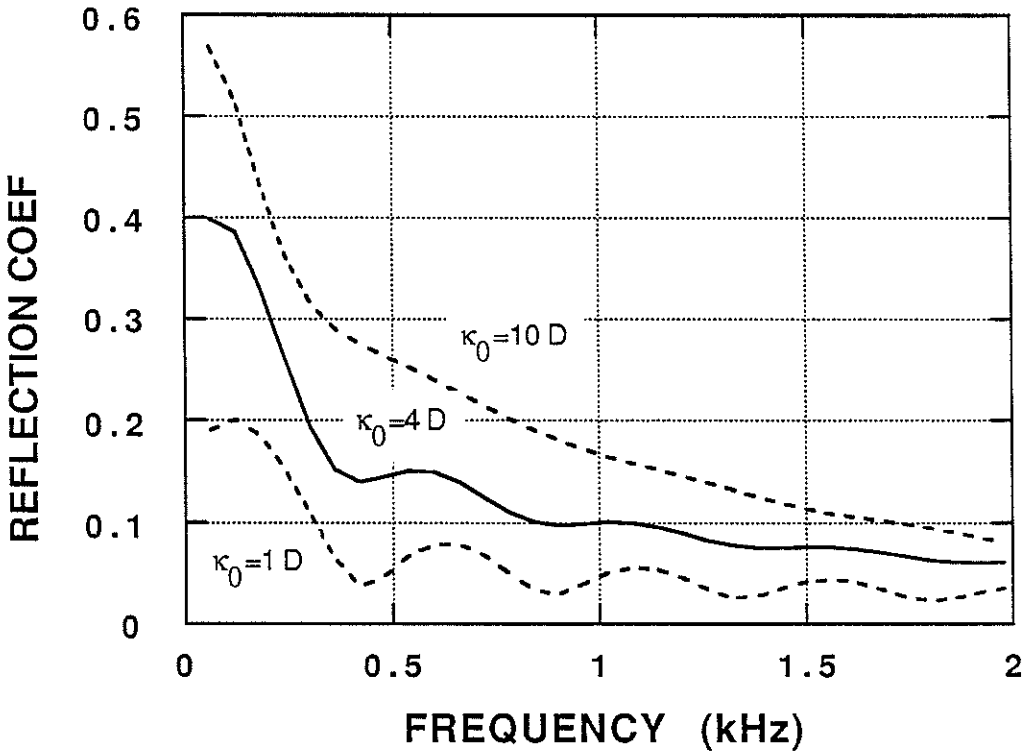


Figure 3: Reflection coefficient due to three different permeabilities. The curve with $\kappa_0$=4 Darcies matches the measured value of 0.1 around 1 kHz. This value is chosen to be the average permeability for the Moodus #1 well.

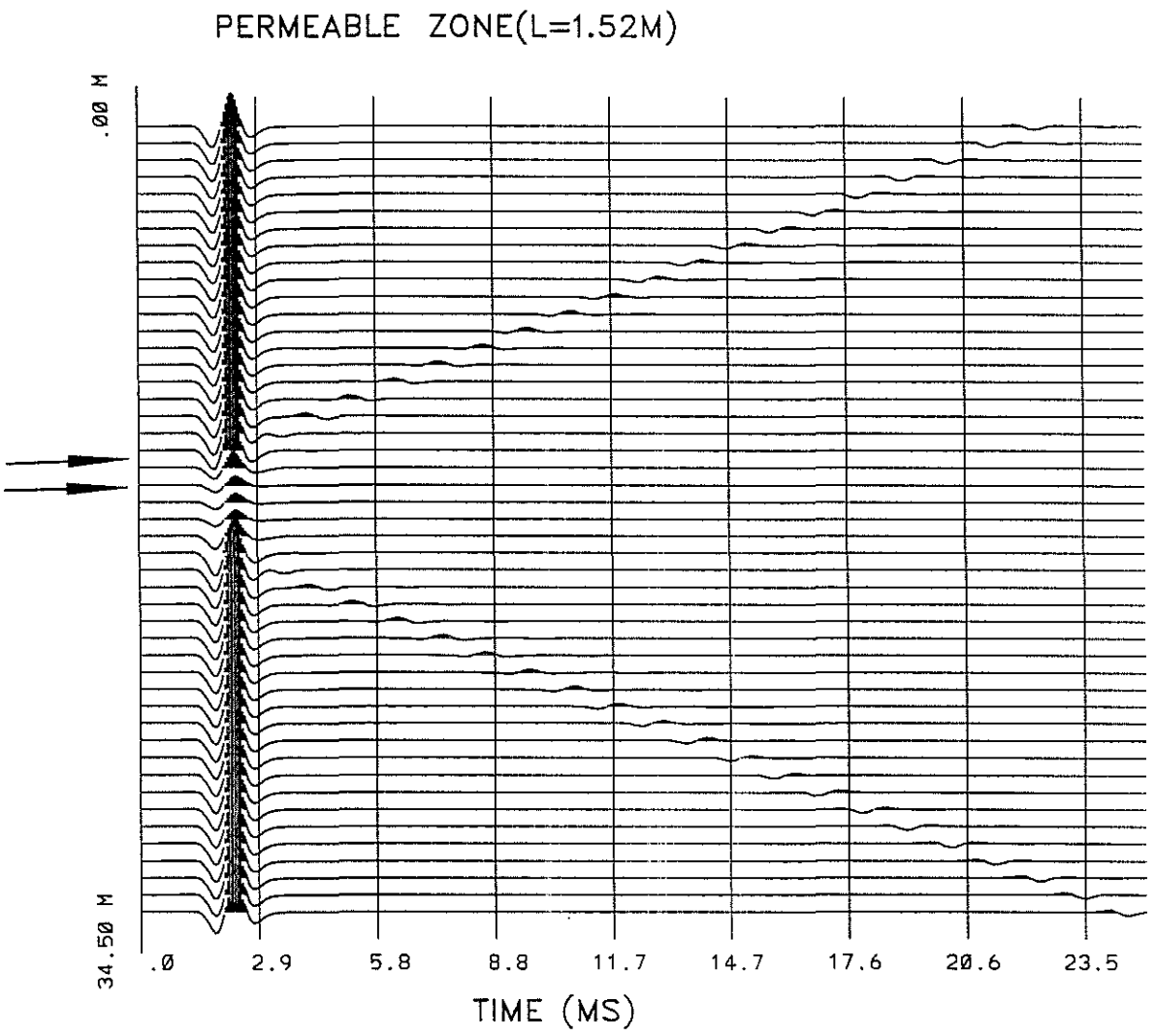


Figure 4: Synthetic iso-offset Stoneley seismograms across the Moodus #1 well fracture zone. The waves are calculated using the permeable zone theory. In addition to the reflection, significant wave attenuation is also predicted, which is consistent with the Stoneley data on Figure 2.

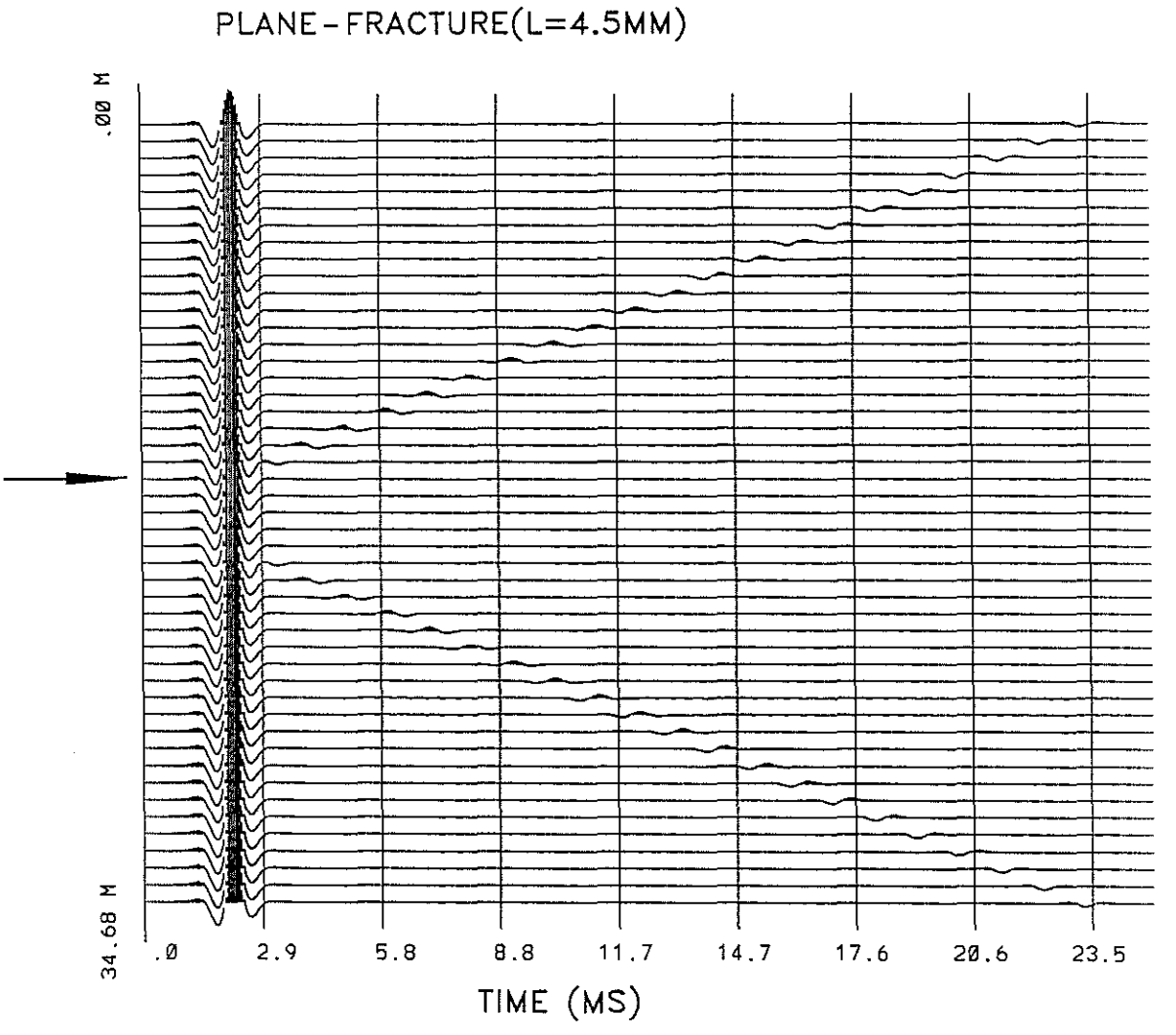


Figure 5: Synthetic seismograms for the Moodus #1 well fracture zone, calculated using the plane-fracture theory. Although the reflection is similar to that of the permeable zone theory (Figure 4), wave attenuation is not recognizable.

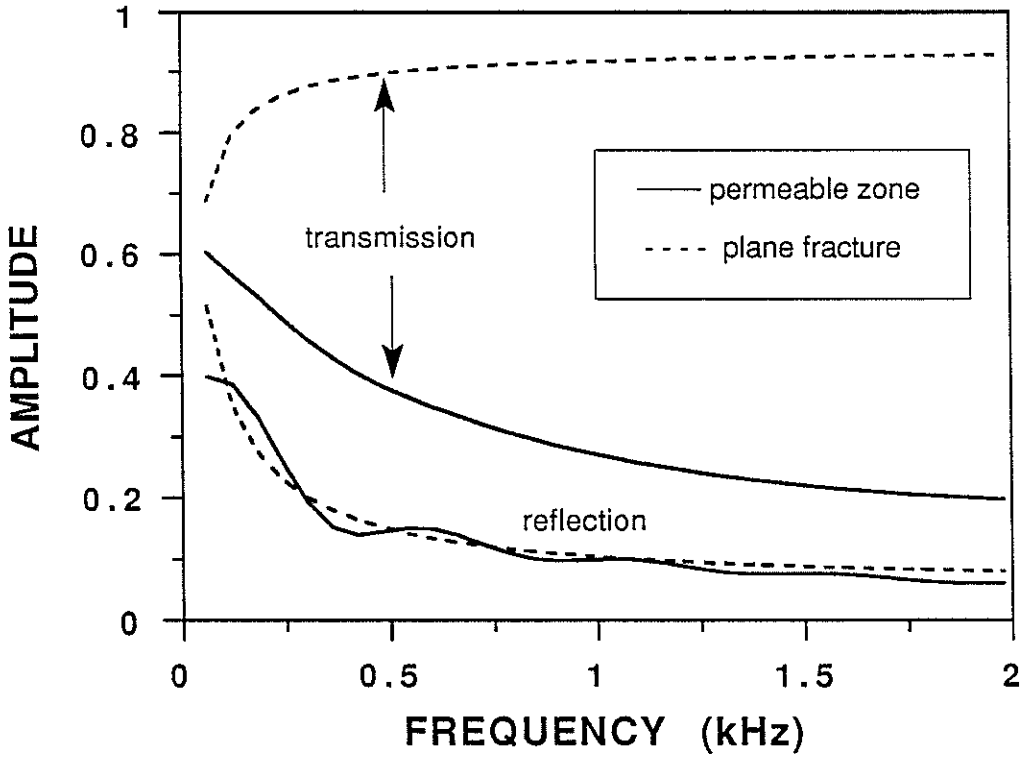


Figure 6: Comparison of the transmission and reflection coefficients of the permeable zone theory (solid curves) with those of the plane-fracture theory (dashed curves). Although the reflections from the two theories match, the transmissions differ greatly.

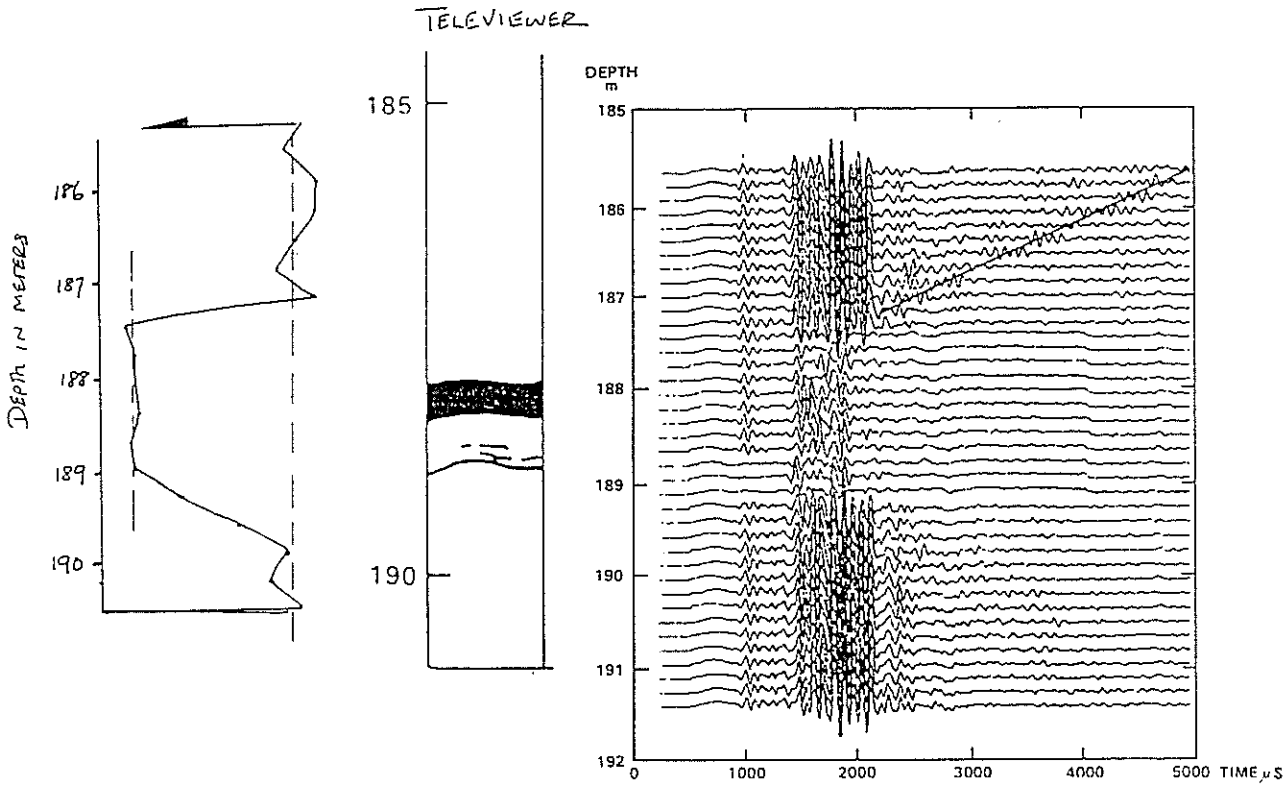


Figure 7: Stoneley waveforms, amplitude log, and televiewer log for the URL-M11 well around 187 m (After Paillet, 1984). The Stoneley reflection and attenuation are evident from this figure.

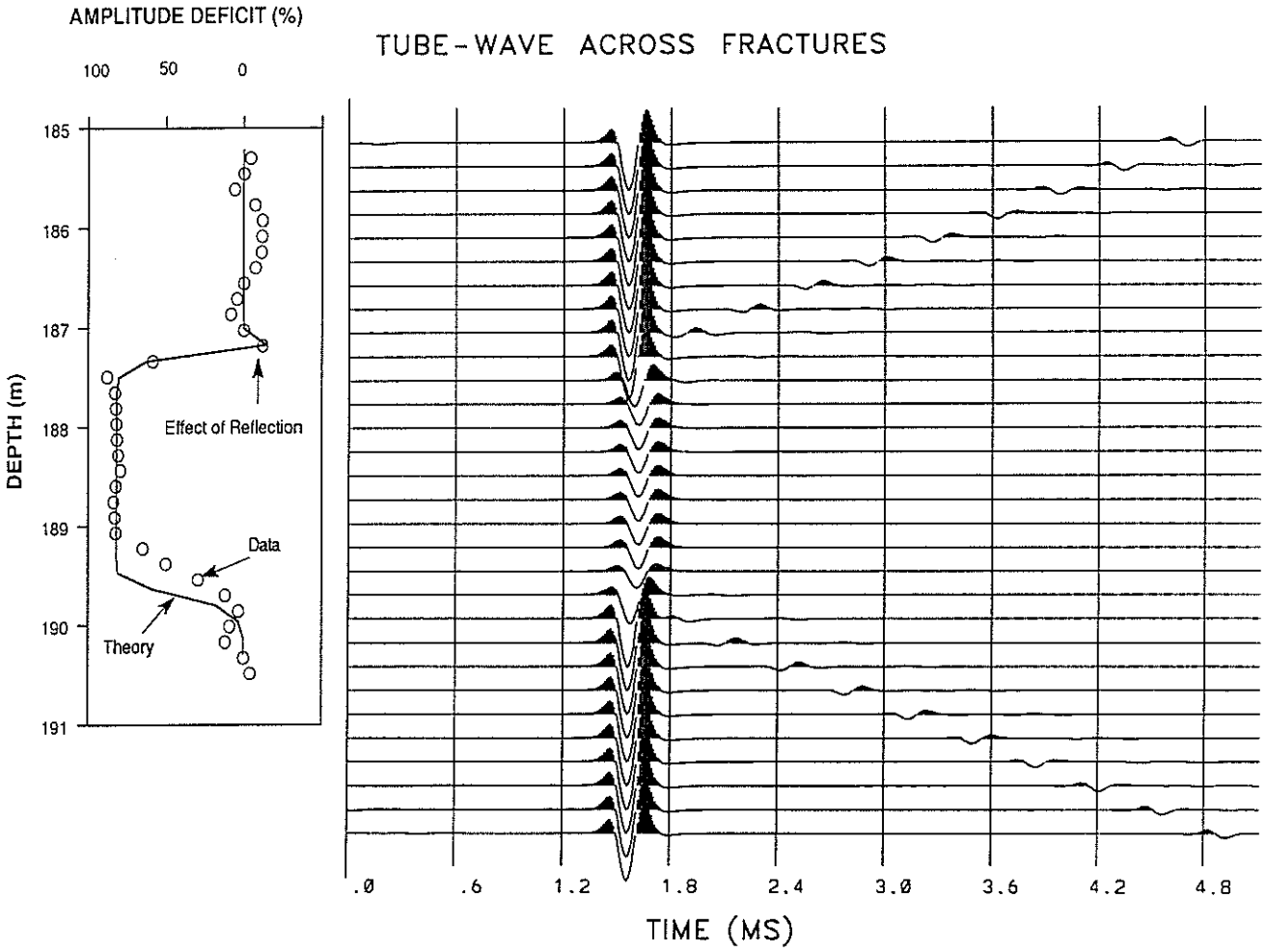


Figure 8: Synthetic Stoneley waveforms across the fracture zone (The logging tool is pulled up from below the fracture). The reflection is predicted and the attenuation, as measured by the amplitude deficit log (solid line), matches the data quite well. Note that the little spike at the top of the amplitude anomaly is due to the interference of the incident and the reflected waves.

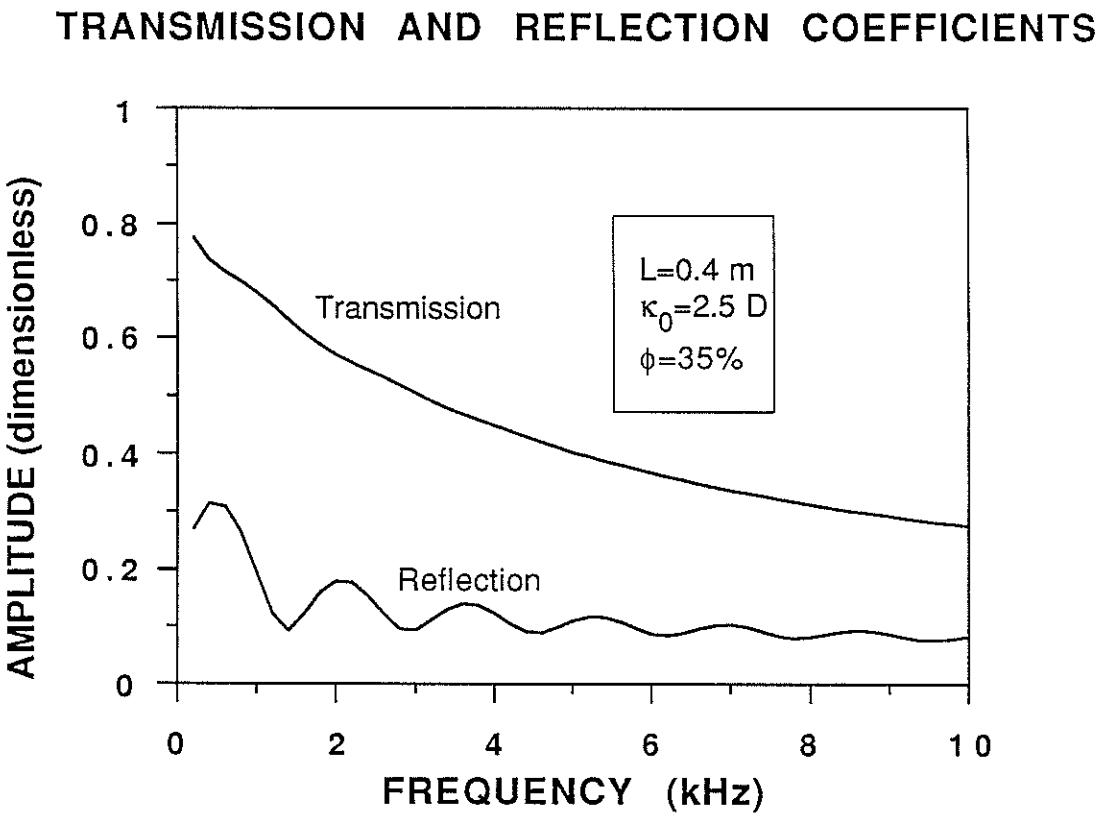


Figure 9: Transmission and reflection coefficients for the URL-M11 fracture zone. The transmission loss is primarily due to fracture permeability, while the reflection is due to both the fracture permeability and the lithology change of the altered rocks in the zone.

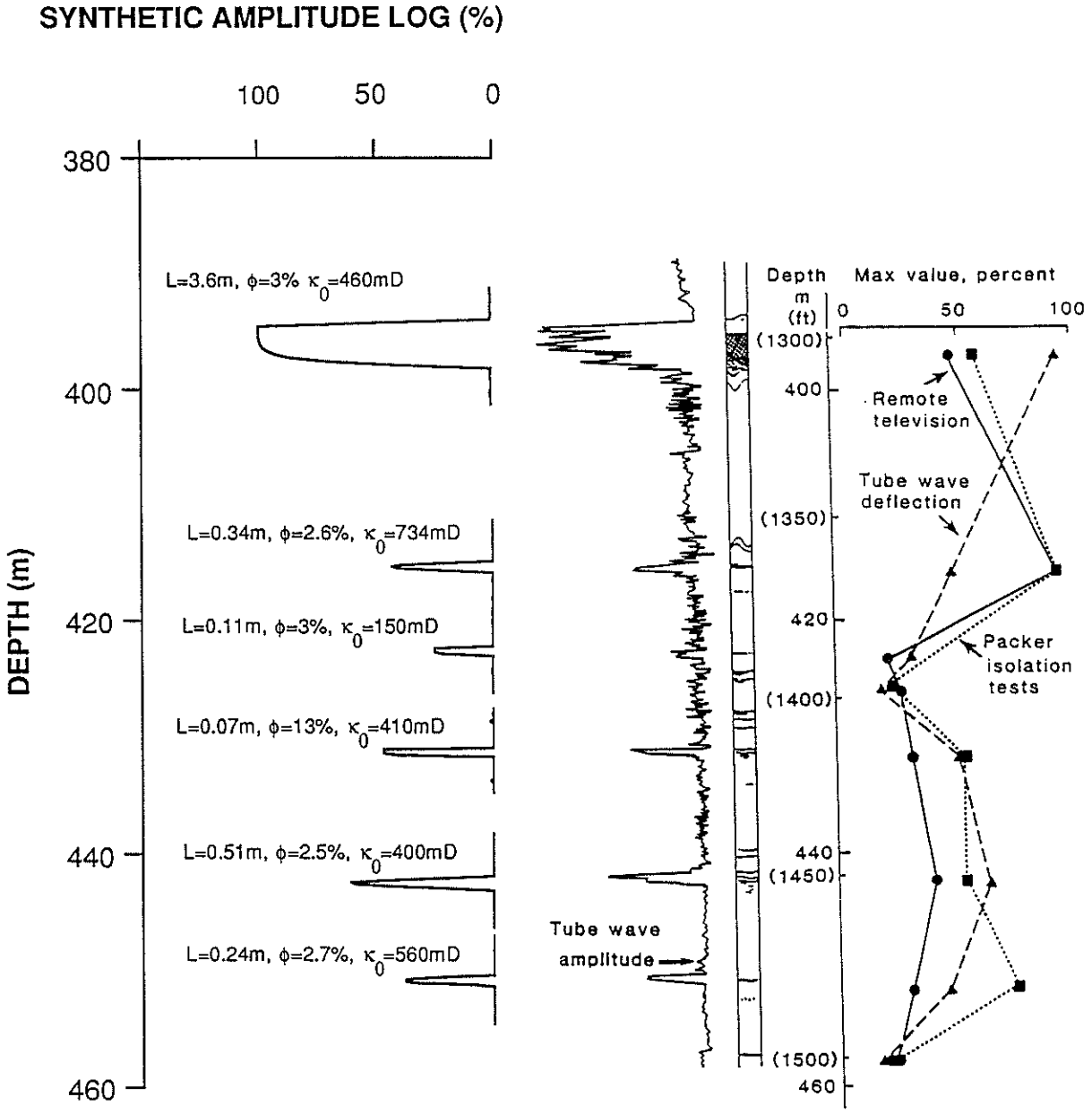


Figure 10: Stoneley amplitude log, televiewer log, and packer isolation results for the Manitoba fracture data set. On the left shows the synthetic amplitude log. From the anomalies on the log, fracture zone thickness $L$ and fracture porosity $\phi$ can be estimated. The permeability numbers are from the packer test, but they do not affect the synthetic result of this high-frequency (34 kHz) data set.

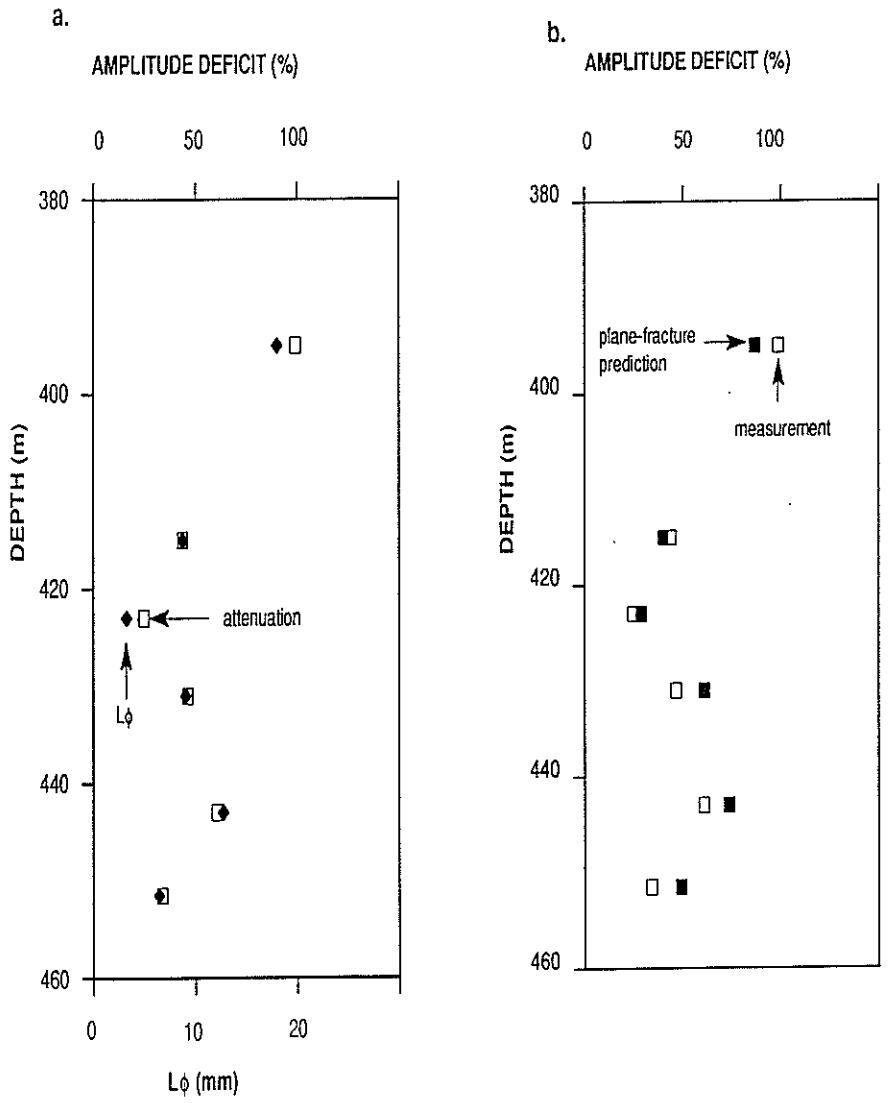


Figure 11: (a) Comparison of the product $L\phi$ with attenuation, which shows that the high-frequency Stoneley attenuation is controlled by $L\phi$. (b) Prediction of attenuation using the plane-fracture theory, in which the fracture thickness is the $L\phi$ values of (a). The agreement of the prediction with the data shows that high-frequency Stoneley waves measure the integrated effects of the fluid-saturated fracture layers.